AD-A277 462



Final Technical Report

on

# TURBULENT REACTING FLOWS AND SUPERSONIC COMBUSTION

Grant AFOSR-90-0151

Prepared for

AIR FORCE OFFICE OF SCIENTIFIC RESEARCH

For the Period

15 February 1990 to 14 October 1993



Submitted by

C. T. Bowman
R. K. Hanson
M. G. Mungal
W. C. Reynolds



HIGH TEMPERATURE GASDYNAMICS LABORATORY
Mechanical Engineering Department
Stanford University

Best
Available
Copy

Approved for public release; distribution unlimited

# REPORT DOCUMENTATION PAGE

Form Approved
OMB No. 0704-0188



**1. AGENCY USE ONLY** *(Leave blank)*

**2. REPORT DATE**
12/15/93

**3. REPORT TYPE AND DATES COVERED**
Final Technical Report

**4. TITLE AND SUBTITLE**
Turbulent Reacting Flows and Supersonic Combustion (U)

**5. FUNDING NUMBERS**
PE - 61102F
PR - 2308
SA - BS
G - AFOSR 90-0151

**6. AUTHOR(S)**
C. T. Bowman, R. K. Hanson, M. G. Mungal, W. C. Reynolds

**7. PERFORMING ORGANIZATION NAME(S) AND ADDRESS(ES)**
Stanford University
Department of Mechanical Engineering
Stanford, CA 94305

**8. PERFORMING ORGANIZATION REPORT NUMBER**
AFOSR-TR- 94 0080

**9. SPONSORING/MONITORING AGENCY NAME(S) AND ADDRESS(ES)**
AFOSR/NA
110 Duncan Avenue, Suite B115
Bolling AFB, DC 20332-0001

**10. SPONSORING/MONITORING AGENCY REPORT NUMBER**

**11. SUPPLEMENTARY NOTES**

**12a. DISTRIBUTION/AVAILABILITY STATEMENT**
Approved for public release; distribution is unlimited
Approved for public release; distribution unlimited.

**12b. DISTRIBUTION CODE**

**13. ABSTRACT** *(Maximum 200 words)*

An experimental and computational investigation of supersonic combustion flows has been carried out. The principal objective of the research was to gain a more fundamental understanding of mixing and chemical reaction in supersonic flows. The research effort comprised three inter-related elements: (1) an experimental study of mixing and combustion in a supersonic plane mixing layer; (2) development of laser-induced fluorescence techniques for time-resolved multidimensional imaging of species concentration, temperature, velocity and pressure; and, (3) analyses and numerical simulations of compressible reacting flows. The specific objectives and results of the research of each of these program elements are summarized in this report.

**14. SUBJECT TERMS**
Supersonic Combustion, Turbulent Reacting Flows, Shear Layers, Laser Diagnostics

**15. NUMBER OF PAGES**
29

**16. PRICE CODE**

| 17. SECURITY CLASSIFICATION OF REPORT | 18. SECURITY CLASSIFICATION OF THIS PAGE | 19. SECURITY CLASSIFICATION OF ABSTRACT | 20. LIMITATION OF ABSTRACT |
|---|---|---|---|
| Unclassified | Unclassified | Unclassified | UL |

# TABLE OF CONTENTS

# 1.0 SUMMARY

An experimental and computational investigation of supersonic combustion flows has been carried out. The principal objective of the research was to gain a more fundamental understanding of mixing and chemical reaction in supersonic flows. The research effort comprised three inter-related elements: (1) an experimental study of mixing and combustion in a supersonic plane mixing layer; (2) development of laser-induced fluorescence techniques for time-resolved multidimensional imaging of species concentration, temperature, velocity and pressure; and, (3) analyses and numerical simulations of compressible reacting flows. The specific objectives and results of the research of each of these program elements are summarized in this report.

## 2.0 INTRODUCTION

Air-breathing propulsion systems offer the potential of higher performance than conventional rocket engines for hypersonic flight. To realize this potential, new combustor design concepts are required. In particular, in order to minimize losses associated with strong shock waves and high combustor inlet temperatures, it is desirable to maintain high flow velocities in the combustion chamber. This design concept leads to a new class of propulsion devices where combustion takes place in supersonic flow.

Combustion in supersonic flow is fundamentally different from combustion in the subsonic flow regime employed in all currently-operating aircraft engines. Many of the design approaches developed over the years for subsonic combustors, e.g., ignition and flame stabilization techniques, are not applicable to supersonic combustion devices, and the current understanding of the fundamental aspects of supersonic combustion is inadequate to support development of these devices.

Recent advances in diagnostic capabilities and significant improvements in our ability to compute such flows offer new opportunities to obtain needed fundamental understanding of compressible turbulent reacting flows. To achieve this understanding, we have carried out a closely-coordinated experimental and computational program that utilized state-of-the-art experimental techniques and computational methods.

The principal objective of the research is to gain a more fundamental understanding of the flow physics and chemistry interactions in compressible turbulent reacting flows. The project comprised three inter-related efforts: (1) an experimental study of mixing and combustion in supersonic flows, (2) development of laser-induced fluorescence techniques for time-resolved multidimensional imaging of species concentration, temperature, velocity and pressure in supersonic flows, and (3) simulation and modeling of supersonic flows with mixing and chemical reaction. A close coupling of these efforts was maintained in order to maximize our understanding of compressible turbulent reacting flows, with an emphasis on supersonic combustion. The specific objectives and results of the research of each of the program elements are described in the following sections.

## 3.0 MIXING AND REACTION IN SUPERSONIC FLOW

### 3.1 Objectives

The objectives of this part of the program are (1) the experimental study of mixing and chemical reaction in a compressible mixing layer and (2) investigation of mixing enhancement in supersonic shear layers. The data acquired, using conventional and laser-based diagnostics, provide important new insights into mixing and reaction processes under compressible conditions.

### 3.2 Research Results

Important experimental results from this aspect of the program are summarized below.

#### 3.2.1 Reacting Flow Studies

Reacting flow experiments were initiated in December of 1991. Work has been focused primarily in three areas: (1) determination the ignition behavior of the mixing layer as a function of the vitiated-air stream temperature, vitiated-air stream oxygen mole fraction and fuel stream hydrogen mole fraction, (2) visualization of the mixing layer structure under conditions of high and low compressibility using planar laser-induced fluorescence (PLIF) imaging techniques and (3) assessment of the effects of compressibility on combustion. The results of the PLIF visualization experiments will be discussed in this section. A complete discussion of the combustion experiments will be contained in the Ph.D. thesis of M. F. Miller (1994).

The nominal free stream conditions for the experiments discussed in this section are shown in Fig. 1. The mixing layer is formed between a supersonic, high-temperature, vitiated-air stream and a subsonic, ambient-temperature fuel stream. The fuel stream consists of hydrogen diluted in nitrogen or helium. Ignition occurs spontaneously in the mixing layer by virtue of the high temperature of the supersonic stream; no ignition device is used. For the results discussed here, the level of compressibility is controlled by the high-speed stream Mach number.

The goal of the PLIF visualization experiments was to determine the effect of compressibility on the structure of the mixing layer. Scalar mixing experiments (Clemens and Mungal, 1992a) and computational investigations (Sandham and Reynolds, 1991a; Planche and Reynolds, 1992) have found that the structure of the mixing layer transitions from a primarily two-dimensional structure to a more three-dimensional structure as compressibility increases. The implications of this observation for reacting mixing layers are immediately apparent. For example, changes in the large-scale structure induced by compressibility changes in the relative entrainment rates of fuel and oxidizer from the free streams as well as may produce changes in the strain-rates in the mixing layer. The observation of structural changes induced by compressibility were the primary motivation for PLIF imaging of the reacting mixing layer.

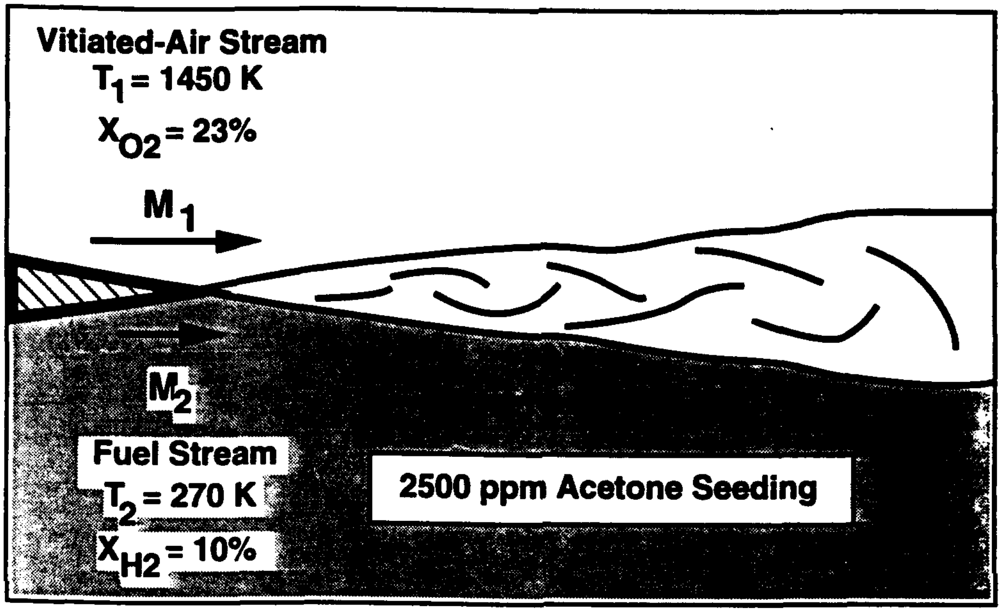


**Fig. 1. Mixing layer free stream conditions.**

A combined OH/acetone PLIF imaging technique is used to visualize the reacting mixing layer (Miller et al., 1993a; Yip et al., 1993). This technique, which was developed under separate AFOSR support with R. K. Hanson as the principal investigator, provides simultaneous images of regions of combustion, marked by OH, and regions of unburned fuel, marked by acetone which has been seeded into the fuel stream. The imaging setup is shown schematically in Fig. 2. A single pulse from a UV laser excites both the OH and acetone in the flow, and the fluorescence signals are detected on separate intensified CCD cameras. Since OH fluoresces in the ultraviolet and acetone fluoresces in the visible, optical filtering can be used to discriminate the signals. There are several reasons why this technique was chosen: Both OH and acetone produce strong fluorescence signals which are essential to obtain high signal-to-noise images suitable for quantitative flowfield interpretation. Additionally, acetone's strong fluorescence signals allow the use of low seeding levels; thus, the perturbation to the flow is minimized. Since this is a large-scale facility, seeding of fluorescent tracers is difficult; however, the low required acetone seeding levels combined with the simple method of seeding acetone into the fuel stream (liquid acetone is sprayed directly into the flow through a fine atomizing nozzle) resulted a workable system. Finally, since only a single laser is required to excite both OH and acetone, the complexity and cost of the imaging system is substantially reduced.

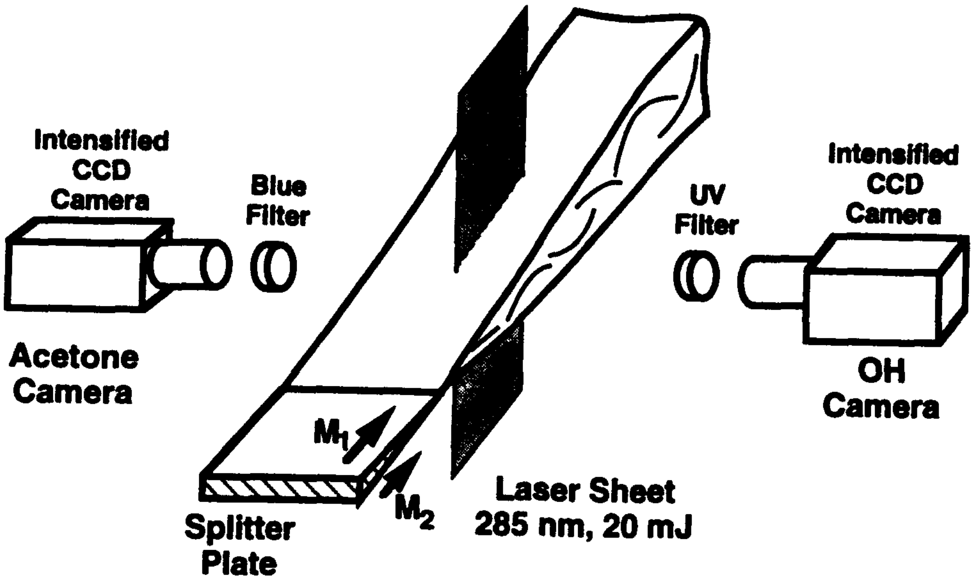


**Fig. 2. Combined OH/acetone PLIF imaging setup.**

As part of the effort to develop and apply the combined OH/acetone PLIF imaging technique to this flow, it was necessary to develop an understanding of the chemical kinetic and spectroscopic behavior of both OH and acetone to facilitate the interpretation of the images. An analysis of acetone and OH for the range of conditions in these experiments was performed (Miller et al., 1993a; Yip et al., 1993). The key results of the analysis of acetone are: pyrolysis is not a significant mechanism for removal of acetone; acetone fluorescence is relatively insensitive to temperature or quenching environment and therefore is proportional to concentration; and, the rates of removal of acetone by radical attack are similar to those of hydrogen. Based on these results, it can be concluded that acetone fluorescence signal is a reasonable marker of unburned hydrogen concentration in the mixing layer. Estimates of OH quenching as a function temperature and composition (ignoring the presence of combustion radicals) indicate that the quenching rate does not vary by more than 20% across the mixing layer. Therefore, the OH fluorescence signals are approximately proportional to OH concentration. The chemical rates of formation and destruction of OH are of the same order as the rates of mixing (strain-rates) in the mixing layer, indicating that OH will be far from equilibrium throughout the flowfield. Hence, OH cannot be interpreted as marking only zones of chemical reaction, rather, OH marks both regions of chemical reaction and regions of hot combustion products.

The experimental conditions for the imaging results discussed below are summarized in Table 1. A high- and low-compressibility reacting mixing layer will be compared. The free stream conditions were maintained as close as possible to isolate only the change in compressibility between the two cases, which is quantified by the convective Mach number, $M_c$.

**Table 1. Experimental Conditions**

| | **High-Compressibility $M_c = 0.70$** | | **Low-Compressibility $M_c = 0.32$** | |
|---|---|---|---|---|
| | Vitiated-Air Stream | Fuel Stream | Vitiated-Air Stream | Fuel Stream |
| Total Temperature [K] | 1800 | 285 | 1590 | 280 |
| Mach Number | 1.25 | 0.41 | 0.70 | 0.53 |
| Static Temperature [K] | 1450 | 276 | 1480 | 265 |
| Velocity [m/s] | 960 | 150 | 540 | 185 |
| Molar Composition | $X_{O2}$ = 23% $X_{H2O}$ = 25% $X_{N2}$ = 52% | $X_{H2}$ = 10% $X_{N2}$ = 90% | $X_{O2}$ = 22% $X_{H2O}$ = 24% $X_{N2}$ = 54% | $X_{H2}$ = 10% $X_{HE}$ = 90% |

Test Section Static Pressure = 0.88 atm

The upper frame of Fig. 3 shows a side-view image of the time-averaged ultraviolet emission from the high-compressibility reacting mixing layer for the first 16 cm of the test section. The splitter tip is at the left-hand edge of the image. The flame stand-off distance from the splitter tip is approximately 5 cm, an indication that the rate at which the combustion is proceeding in this flow is comparable to the fluid mechanical mixing and convection rates. The two lower frames contrast the time-averaged ultraviolet emission (on the left in blue), and the instantaneous OH PLIF (on the right in yellow); both images are side-views (8 cm wide and 5 cm high) obtained at an imaging location centered 22 cm downstream of the splitter tip. This comparison is a convincing demonstration of the ability of instantaneous PLIF imaging techniques to reveal the details of the flow which are lost in time-average measurements.

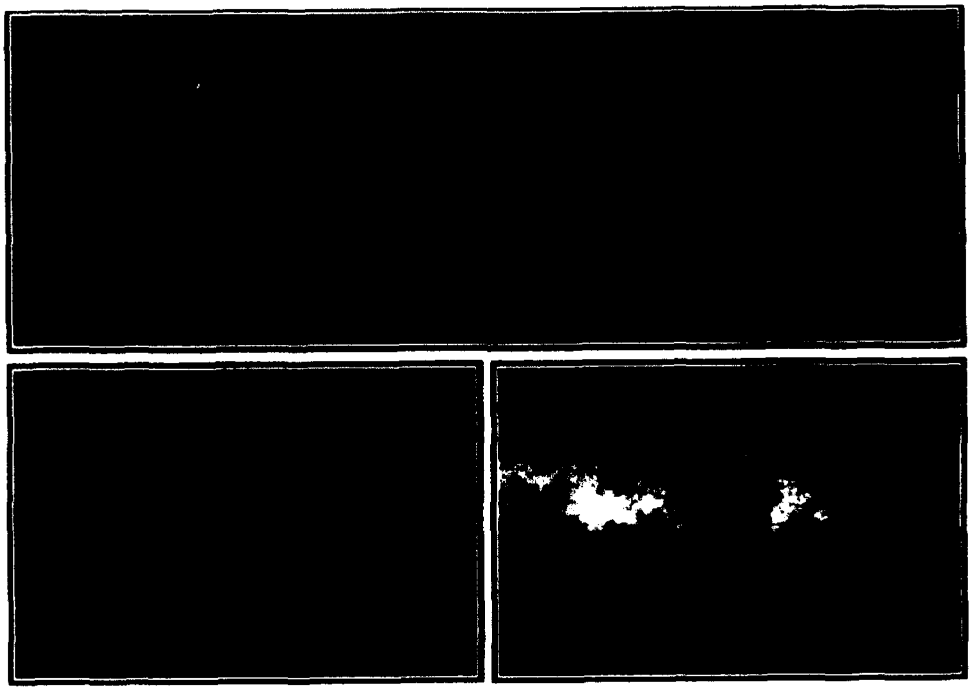

Fig. 3. Side-view images of the $M_c$ = 0.70 reacting mixing layer. Upper frame: Time-averaged ultraviolet emission from the first 16 cm of the test section. The splitter tip is at the left-head edge of the image. Lower frames: Time-averaged ultraviolet emission from 18 cm to 26 cm (left). Instantaneous OH PLIF at same imaging location (right).

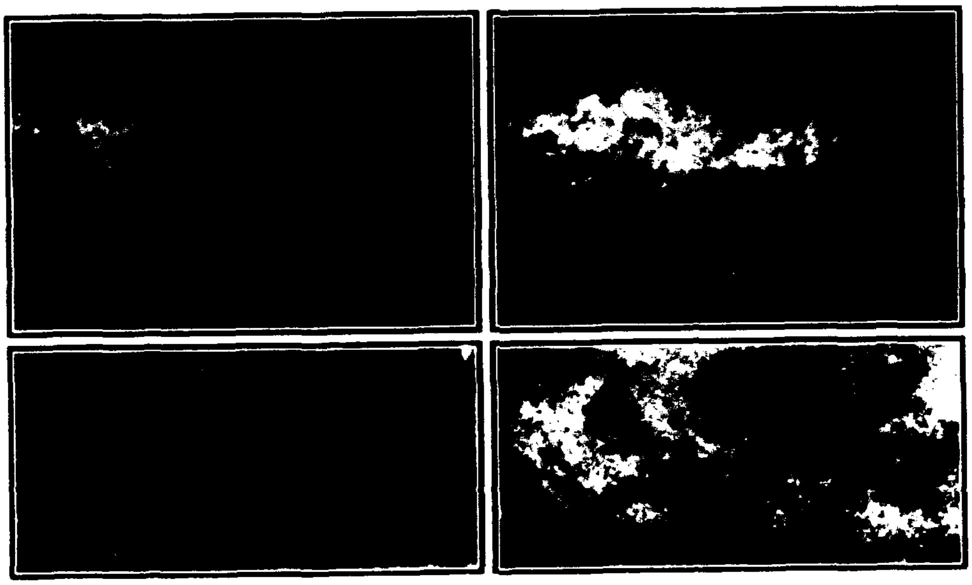

Fig. 4. Instantaneous OH/acetone PLIF images of reacting mixing layer. Upper frames are side views; the lower frames are plan views. $M_c$ = 0.32 case is shown on the left, and $M_c$ = 0.70 case is shown on the right.

The combined OH/acetone PLIF images of both the high- and low-compressibility reacting mixing layers in side- and plan-view are show in Fig. 4. The OH PLIF signals are displayed in yellow, and the acetone PLIF signals are displayed in purple. For the side-view images, the region of high signals at the bottom of the images is the low-speed free stream (acetone bearing fuel stream). Lower levels of acetone indicate fuel which has been entrained into the mixing layer, diluted and possibly reacted. The combined OH/acetone images reveal that the spatial extent of the reacting mixing layer is greater than that which was indicated by the time-averaged emission or the instantaneous OH PLIF images shown in Fig. 3, illustrating the utility of simultaneous acquisition of multiple scalar fields. Also apparent from these images is that high signals levels of OH and of acetone in the mixing layer are mutually exclusive. This observation indicates that combustion is occurring in the hot, fuel-lean zones of the mixing layer while the remainder of the mixing layer is composed of cool, fuel-rich zones.

The purpose of the PLIF visualization experiments was to investigate the effect of compressibility on the structure of the mixing layer. The low-compressibility mixing layer structure should be dominated by two-dimensional, spanwise vortical structures seen in previous nonreacting experiments (Clemens and Mungal, 1992a). The combined OH/acetone PLIF side- and plan-view images of the low-compressibility mixing layer shown in Fig. 4 show clear evidence of this structure. The clearest evidence is provided by the plan view image which shows a "banded" structure where the OH and acetone signals appear in predominantly spanwise uniform regions. The high-compressibility mixing layer images do not show this distinct structure. The side-view image has a more disorganized structure, and the plan-view does not possess the banded structure of the low-compressibility case. The high-compressibility case shows a distinct increase in the three-dimensionality of the flow.

The combined OH/acetone PLIF technique has also been applied to these flows in a double-pulsed mode where two sets of simultaneous OH and acetone PLIF images are obtained at two time intervals separated by approximately 50 μsec (Seitzman et al., 1994). The purpose of these experiments was to measure the convective speeds of structures from the image pairs and to gain some insights into the temporal evolution of the structures at different levels of compressibilities. Analysis of the combined OH/acetone PLIF imaging results is still in progress with the continuing goal of elucidating the effect of compressibility on the combustion; however, the utility of the measurements obtained to date is clearly evident from results discussed above.

### 3.2.2 Mixing Enhancement Studies

The stability analyses and direct numerical simulations, performed to date, have suggested ways in which to enhance mixing in compressible mixing layers utilizing controlled introduction of streamwise vorticity. Hence, a second aspect of our work involved preliminary investigation of three different strategies for mixing enhancement: discrete vortex generators and jets, Side Wall Shock Vortex Generators (SWSVG), and moderate unstable streamwise curvature. Each of these approaches shares the common element that it attempts to introduce streamwise vorticity perturbations, to which the flow is receptive. Instability mechanisms of the flow will amplify the disturbances, leading to increased entrainment and consequent mixing. To date, we have performed preliminary studies using SWSVG, streamwise curvature and a fixed vortex generator.

The SWSVG (Clemens & Mungal, 1992b) produced up to a 60% increase in volume of mixed fluid, but with an associated pressure loss penalty. The dramatic changes in the layer suggest that the flow is certainly very receptive to this approach, however no optimization studies have yet been performed. In particular, the mechanism by which the vortex disturbance initiates, grows and amplifies is not yet understood. Our results have also shown that a single vortex generator, attached to the splitter tip, produces about a 45% increase in mixed fluid volume, with associated pressure penalties. In addition to producing a vortex, the physical presence of the vortex generator also produces waves, so that we are unable to ascertain the result of each - vortex vs wave contribution. Finally the Vortex Generator Jet (VGJ), whereby a pitched and skewed jet can be used to directly affect a supersonic cross-flow and increase mixing can be used to resolve the vortex effect versus the wave effect, but has not been tried to date.

One additional approach which has been explored was the use of streamwise curvature, Fig. 5. To date, we have found about a 20% increase in mixed fluid volume with little pressure penalty. Here the strategy is to create a change in the natural instability in the flow that favors the growth of streamwise instabilities. The flow was run only in the "unstable" configuration, i.e. with the high-speed flow on the inside of the curved path. We have previously found up to 50% increase in mixed volume in subsonic flows, and expect a stronger coupling in supersonic flows. We now believe that the 20% finding results from a situation whereby the facility is being run too "clean", with the flow better able to respond to discrete point disturbances of the type described above. Thus while the SWSVG and vortex generator studies can be characterized as "dirty" in terms of the amplitude of the disturbances used, we believe that amplitude control must be exercised, in future, in producing the desired mixing enhancement.

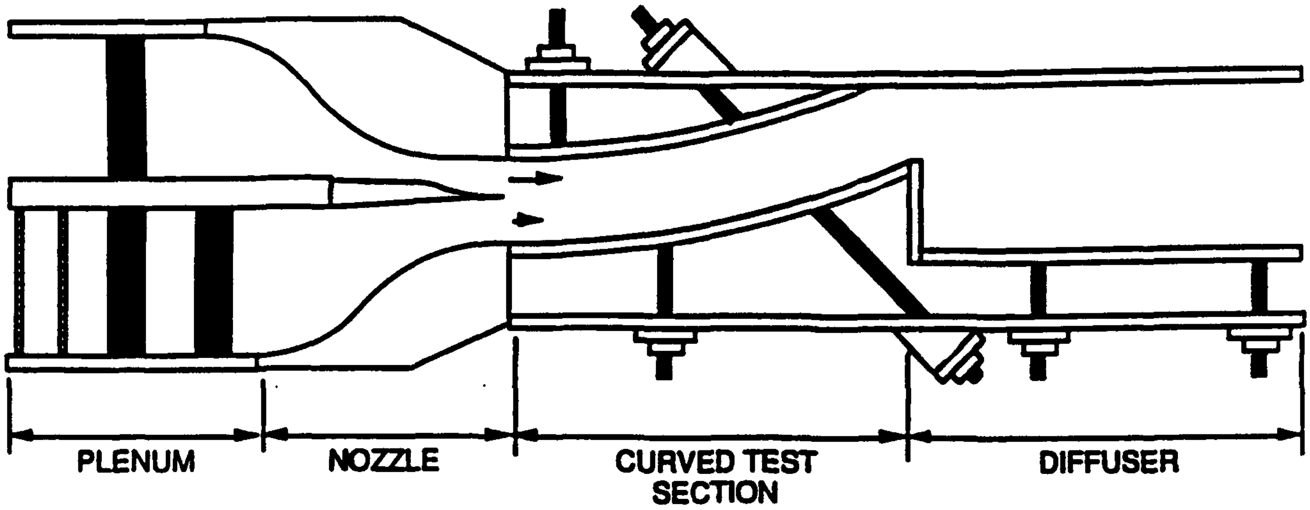


**Fig. 5. Implementation of curved mixing layer for mixing enhancement studies.**

## 4.0 SUPERSONIC FLOW DIAGNOSTICS

### 4.1 Objectives

This element of our research program is aimed at developing flowfield imaging diagnostics based on Planar Laser-Induced Fluorescence (PLIF). Flow parameters of interest include species concentrations (or mole fractions), temperature, velocity and pressure. Particular emphasis is placed on imaging nitric oxide (NO), molecular oxygen ($O_2$) and hydroxyl radicals (OH), since these species are naturally present in most supersonic propulsion flows of interest.

### 4.2 Research Results

Work over this reporting period has been in five areas: (1) flow facility development; (2) code development for method-of-characteristics solutions of nonequilibrium supersonic free jets; (3) PLIF imaging of hypersonic shock tunnel flow; (4) PLIF imaging experiments of shock-induced ignition phenomena; and (5) PLIF imaging of mixing and combustion of transverse jets in shock-generated supersonic flow.

#### 4.2.1 Flow Facilities

There have been three flow facility projects, all associated with the shock tube which was assembled early in this AFOSR program. The primary project has involved design and assembly of a shock tunnel extension to the shock tube. This shock tunnel comprises a dump tank, supersonic free jet test section, and hardware to couple the test section to the existing shock tube. In these experiments, reflected shock waves are used to generate controlled, high temperature and pressure stagnation conditions, causing the gas to flow into the dump tank through a converging nozzle. The result is an underexpanded supersonic free jet with a wide range of temperature, pressure and velocity along the jet centerline. This flowfield is ideal for developing and testing new diagnostics since it: (1) is an economical design (no contoured diverging nozzle needed); (2) provides an extremely wide range of flow conditions in a single flow; and (3) gives good optical access. The flowfield conditions can be chosen to provide varying degrees of nonequilibrium (e.g., vibrational nonequilibrium with separate vibrational and translational/rotational temperatures); this enables important tests of the suitability of various diagnostic strategies to deal with nonequilibrium supersonic flows.

A second facility project involved modifying the planar end wall of the shock tube to include a shallow v-groove. The objective was to provide slightly nonuniform shock wave reflection, leading to localized ignition of shock-heated fuel-oxidizer mixtures.

This facility was useful in developing PLIF imaging strategies suitable for studies of ignition phenomena.

Finally, the third flow facility project entailed modifications to the side wall of the shock tube to incorporate a pulsed valve assembly. This facility provides a convenient capability for studying the mixing and combustion of a transverse jet in a supersonic cross-flow. The low cost of this facility, and the wide range of flow conditions which can be generated, have enabled important research on diagnostics relevant to scramjet phenomena.

4.2.2 Flowfield Codes

During the past three years we have completed work on assembly of a computer code to describe nonequilibrium supersonic free jets. This code is critical to evaluation of the PLIF imaging data acquired in our shock tunnel. The code is able to handle three critical flowfield cases: (1) constant gamma (ratio of specific heats); (2) vibrationally equilibrated flow (infinite relaxation rate); and (3) finite relaxation rate. In each case, the code calculates the entire flow between the nozzle exit (sonic condition) and the Mach disc. An example result showing the variation of temperature along the jet centerline is shown in Fig. 6. In this case, the flow is 100% $O_2$, but several different mixtures involving various proportions of $NO/O_2/N_2/Ar$ are of interest and will be studied. Note that results are provided for both the vibrational and translational/rotational temperatures and for a range of vibrational relaxation rates (frozen flow, finite rate relaxation, and equilibrium flow).

In conducting PLIF imaging of these flows, we have been able to establish strategies for imaging both the vibrational and translational/rotational temperatures as well as velocity and pressure.

4.2.3 PLIF Imaging of Shock Tunnel Flow

Nonequilibrium supersonic/hypersonic flows, relevant to current research on scramjets, pose new measurement problems for experimentalists. For example, experiments are often conducted in pulsed flow facilities in which the available measurement time is quite limited, thereby putting a premium on the ability to acquire complete data sets in very short times. In addition, many flows of interest exhibit a high degree of nonequilibrium, requiring experimental methods sensitive to such effects. PLIF has high potential for dealing with both of these critical problems, in that the data yield densities in specific quantum states of the species probed at a very large number of flowfield locations. During the past five years we have conducted research which addresses the primary problems inherent in extending PLIF to transient supersonic flows. Our strategy has been to employ a shock tube to provide the transient, high-enthalpy, supersonic flows of interest, and these experiments are now yielding important results. Specific accomplishments of the present three-year program, discussed below, include the first applications of PLIF to a shock tunnel flow. Shock tube experimentation with transverse jet injection into a supersonic cross-flow is reported separately in Sec. 4.2.5.

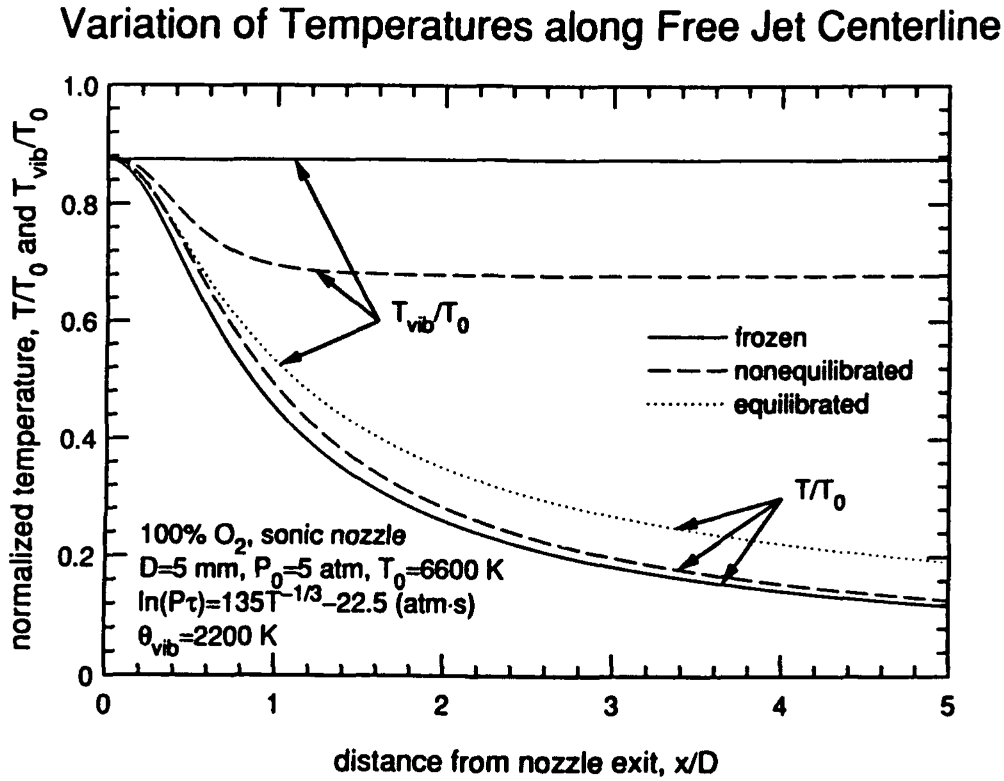


**Fig. 6. Method-of-characteristics solutions for temperature on centerline of an underexpanded free jet with vibrational relaxation.**

Our shock tunnel experiments have been carried out in a standard pressure-driven shock tube, modified to include an exit nozzle in the shock tube end wall which separates the main body of the shock tube and a dump tank. A schematic of the experimental facility including associated optical and electronic components for PLIF imaging is shown in Fig. 7. This facility provides a convenient, economical and highly reproducible means of generating high-enthalpy, underexpanded free jets for a wide range of gas mixtures, jet expansion ratios and stagnation enthalpies. This flowfield exhibits extreme variations in pressure and temperature, as well as high speed and Mach numbers, which render it a challenging and appropriate environment in which to explore and validate PLIF measurement strategies.

Primary objectives of the research during the past three years has focussed on the development of measurement strategies for rotational/translational temperature and velocity. The emphasis has been on NO, since it is generated in many practical high-enthalpy tunnels and, as a stable compound, can be conveniently seeded for use in low temperature flows. As a part of this effort, we have completed a thorough spectroscopic analysis of the NO spectrum in the A←X system, including development of a detailed fluorescence model which predicts the possible effects of rotational energy transfer and saturation phenomena. Here we highlight the experimental portion of the effort, which includes single-shot PLIF imaging of velocity and temperature, and the agreement found between these data and calculations carried out with our MOC code.

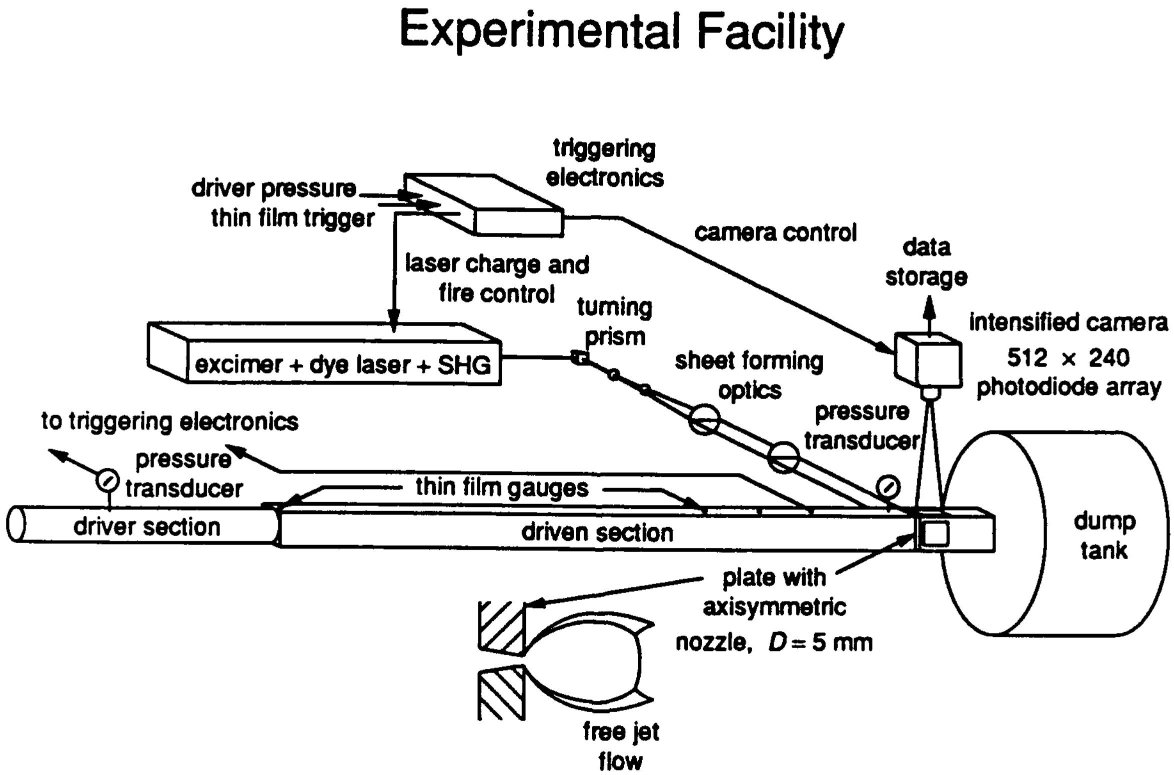


**Fig. 7. Schematic of experimental facility with associated optical and electronic components for PLIF imaging in a shock tunnel.**

The temperature imaging was based on the ratio of fluorescence signals using laser pumping of different rotational states in the v = 0 vibrational level of the ground electronic state of NO. Owing to the wide temperature variation along the jet centerline, no two rotational states provide sensitive temperature determinations over the full extent of the jet. In order to study the influence of the state selected for pumping, we utilized 6 separate absorption transitions with rotational quantum numbers as low as 5 and as high as 28. As expected, the low rotational states provide the strongest signals and best temperature sensitivity in the lower temperature (highest Mach number) region of the jet, just upstream of the Mach disc, while the high rotational states provide the best signals nearer the nozzle exit where temperature is high. The best compromise choice for temperature determination was found to be: the $Q_1 + P_{21}(5)$ and $Q_2 + R_{12}(7)$ transitions (here the splitting of the main Q-branch and satellite transitions is small enough that the lines overlap almost fully and are treated as a single absorption line). Example results showing the temperatures inferred from single-shot and 5-frame-averaged data are given in Fig. 8. The stagnation conditions for this case are: 4200K, 3.0 atm, NO/Ar = 2/98. Even at these relatively low levels of NO, the single-shot signal-to-noise ratio is reasonably good, allowing good resolution of temperature. Note also that the agreement between the MOC code and the data is quite good. Our conclusion from this work is that PLIF imaging of NO in supersonic nonequilibrium flows holds high promise for applications in larger scale facilities used for various forms of propulsion research. Recently we have refined our experimental technique and extended it to include the vibrational temperature (which may differ from the rotational/translational temperature). Details of this work may be found in our publications listed in Section 6.0.

Initial results have also been obtained for velocity using the Doppler-shift concept developed earlier in this laboratory. Data for velocity are acquired by slightly detuning the laser so that the central frequency of the laser line is nonresonant with the absorption line. In this case, the effective laser intensity depends on the local gas velocity component in the direction of illumination. Example single-shot data (for the case of radial illumination, i.e., 90 degrees to the flow axis, the same as used for temperature imaging) and a comparison with MOC calculations are shown in Fig. 8. The flow conditions are the same as noted above for the temperature data. The data have been interpreted using two different algorithms: a simple, linear fit to the laser lineshape; and a more complex, nonlinear fit. For large velocities, above about 600 m/s, it is clear that the nonlinear fit is required. The good agreement between the data and MOC calculation is very encouraging, especially in view of the fact that the data are acquired in a single laser shot. Equivalent results for the axial velocity have been obtained using illumination at other angles.

We have carried out an analysis of the velocity imaging strategy and identified the aspects of the measurement which most need refinement. In particular, we found that key parameters of the laser should be monitored on each shot, particularly the laser energy, spatial distribution (i.e., the "sheet correction"), and the spectral distribution. Recently we have incorporated measurements of variables on a shot-to-shot basis, though further improvement in measurement accuracy is needed for some variables.

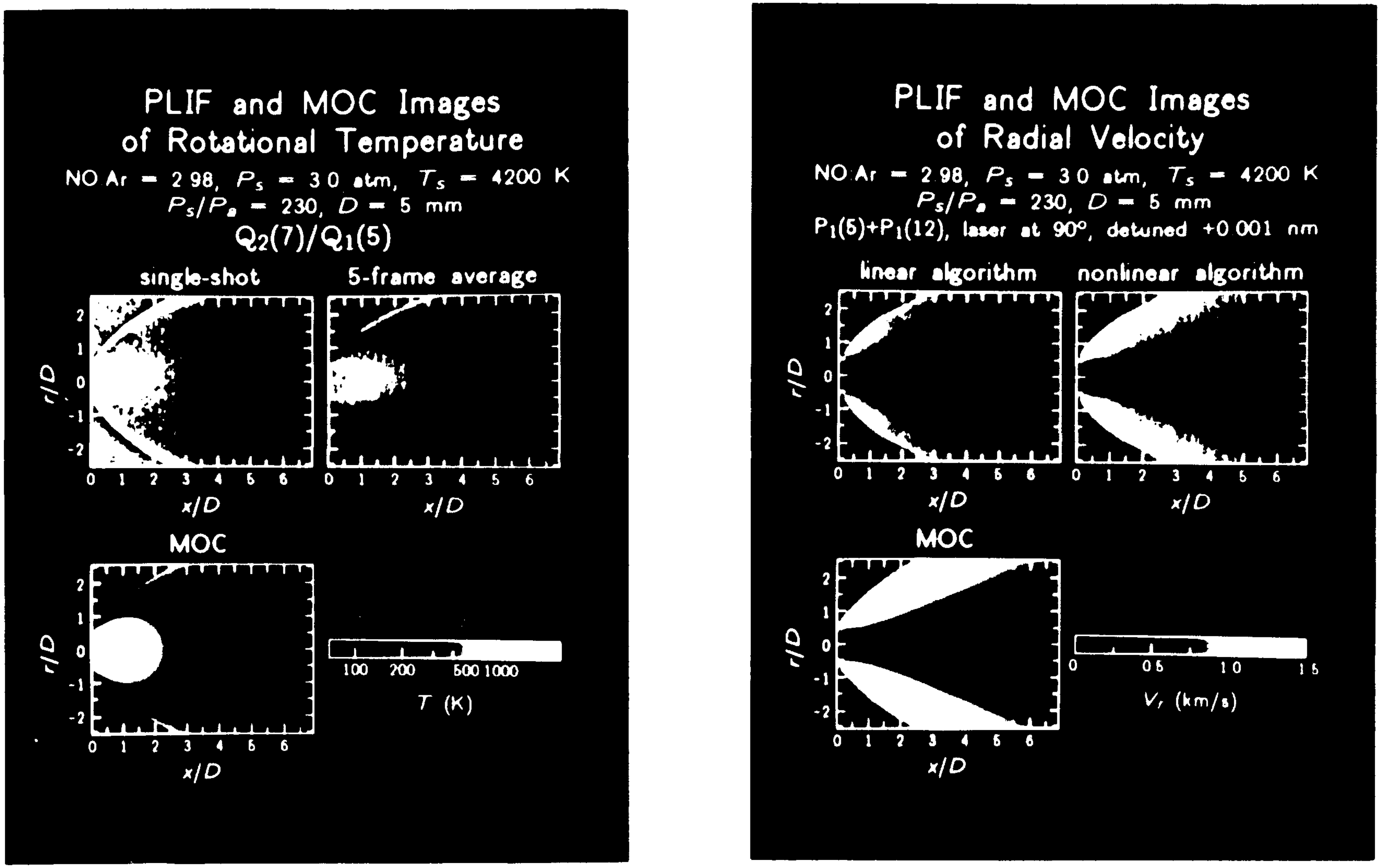


Fig. 8. PLIF imaging results and MOC calculations for a nonequilibrium supersonic free jet; the conditions for the experiment are indicated on the figure.

#### 4.2.4 PLIF Imaging of Shock-Induced Ignition

In this program we have been concerned with developing PLIF imaging strategies suited for monitoring ignition phenomena in $H_2$-$O_2$ mixtures at elevated temperatures. The approach we have taken is to monitor OH production in the region behind a reflected shock wave. The shock tube end wall was modified to include a shallow groove, so that local nonuniformities in post-shock temperature are created after shock reflection. The influence of the resulting temperature variations is to cause localized ignition, which then spreads as a moving flame front, since the ignition reactions are highly temperature sensitive. This flowfield provide an interesting and relevant testing ground for the development of PLIF imaging in reactive flows. Problems encountered and solved include: optimized selection of the laser source, selection of the appropriate OH transition, and several difficulties associated with synchronization of the shock tube, fuel-oxidizer ignition, laser pulse, and intensified camera gating.

Sketches of the experimental arrangement and imaging geometry typically employed are shown in Figs. 9 and 10. Sample results for the case of strong ignition (i.e., relatively high temperature flowfields) are shown in Fig. 11. Results were obtained near both the weak- and strong-ignition limits, with the former showing much greater three-dimensionality, as expected. The results for strong ignition exhibit two-dimensional behavior, as is apparent in Fig. 11. In all these data sets, the images essentially represent the instantaneous mole fraction of OH as produced by the ignition occurring behind the reflected shock wave. Note the emergence of a jet of hot fluid from the groove, leading to a triangle-shaped burned region bounded by nearly straight flame fronts. The forward flame front is co-planar with the reflected shock wave which has moved out of the field of view. Combustion also is apparent in the remainder of the reflected shock zone, but the lower temperatures lead to a slight time delay in this process. Eventually, the combustion fronts merge into a single planar front which moves away from the end wall at a constant flame speed.

#### 4.2.5 PLIF Imaging of Supersonic Jet Mixing and Combustion

A primary objective during this three-year period has been the development of PLIF approaches to the imaging of transverse jets in supersonic cross-flow. In particular, the objective has been to develop methods for imaging critical aspects of the mixing and combustion which occur in such jets; this has included measurements of jet mixture fraction, flame front location, combustion products, and temperature. This gasdynamics problem is highly relevant to current research and development of scramjet engines. Because past measurements in such flows were based exclusively on conventional instrumentation such as pressure gauges, interferometry, schlieren, radiative emission,

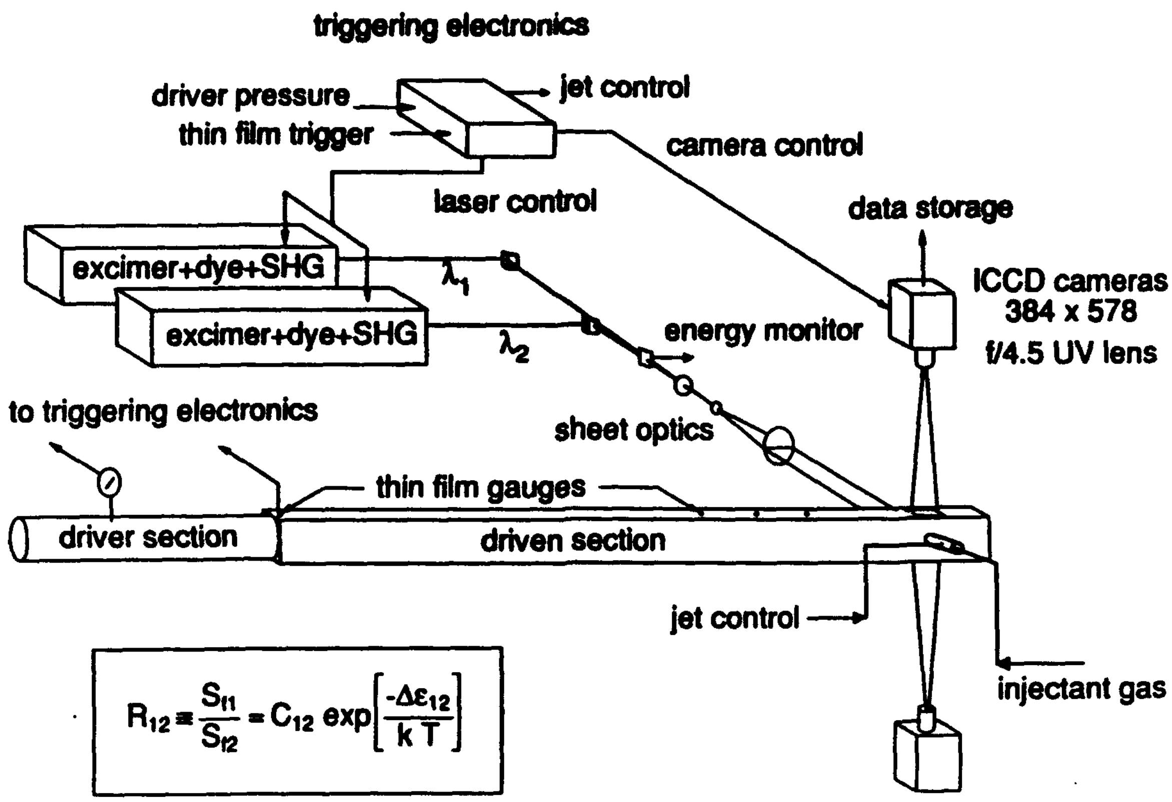


Fig. 9. Schematic of shock tube facility for PLIF imaging.

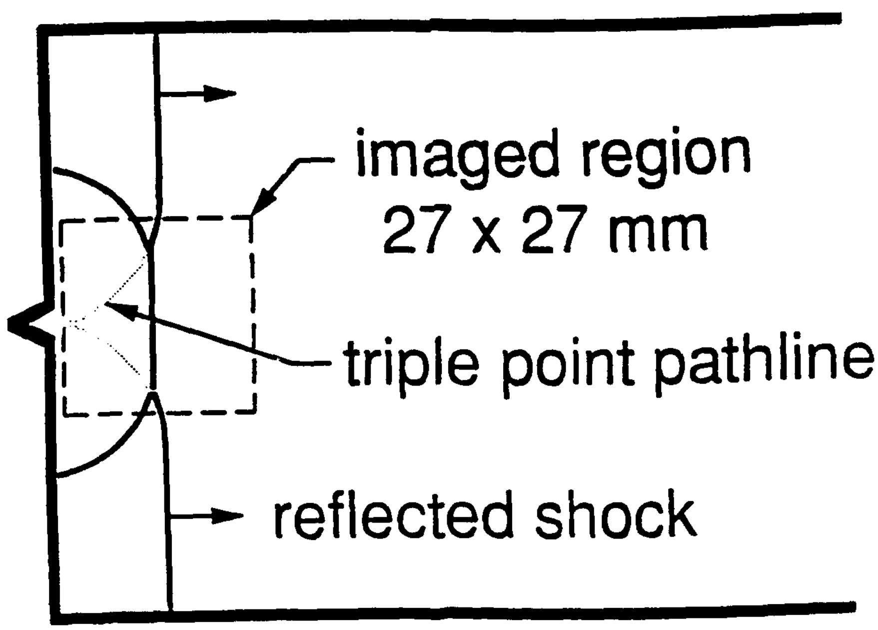


Fig. 10. Schematic of imaging geometry for the endwall with the vertical V-shaped groove down the center. The reflected shock structure a short time after reflection is sketched qualitatively.

Fig. 11a

Fig. 11b

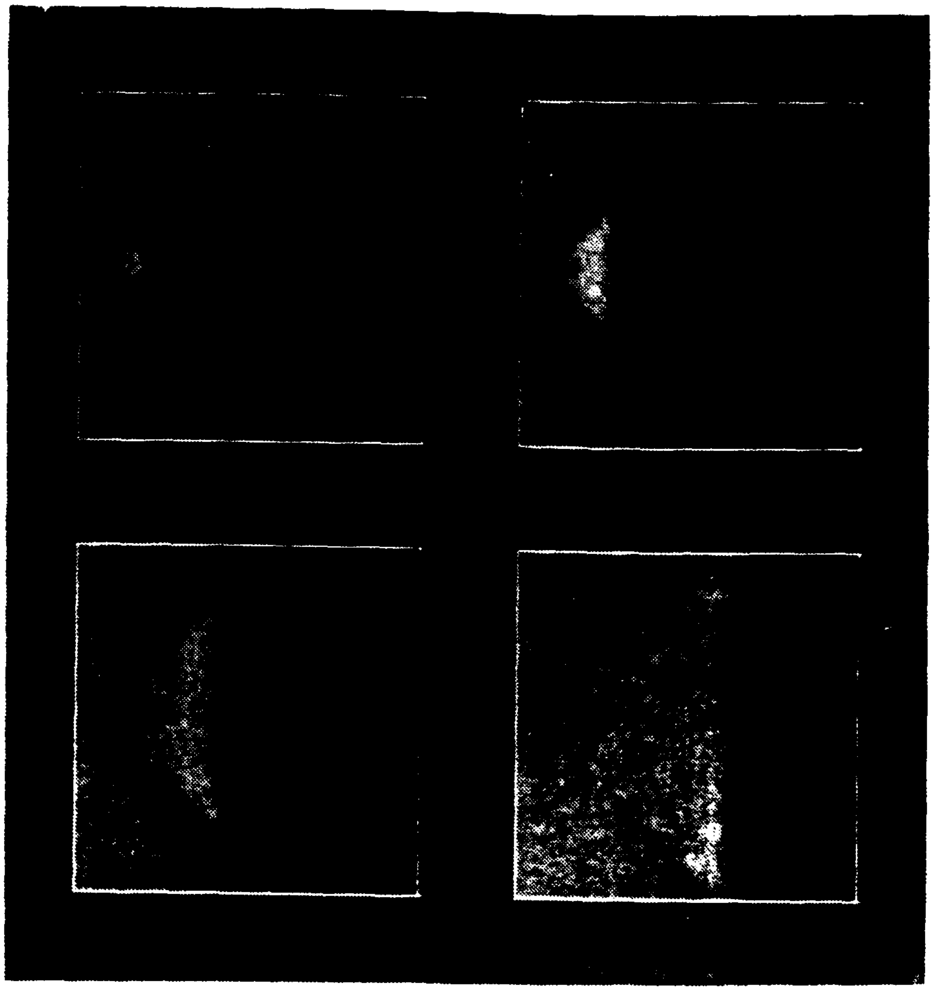

Fig. 11c

Fig. 11d

Fig. 11. Sequence of four PLIF images of OH acquired in the strong ignition limit behind a shock reflected off the V-groove endwall. The image in (a) was acquired ~35 μsec after shock reflection. Images (b), (c) and (d) were acquired in separate experiments at delays of 10, 25 and 45 μsec with respect to (a). Neglecting the effect of the nonplanar endwall, the conditions behind the reflected shock were 1440 K and 1.9 atm and the reflected shock speed was 0.45 mm/μsec.

etc., there is a high potential payoff for the successful development of nonintrusive imaging schemes which can yield some of the properties noted above. In fact, techniques and measurement of strategies successfully demonstrated in this program have already been implemented in other U.S. laboratories active in scramjet development.

In order to provide a meaningful environment which simulates critical aspects of the jet mixing and combustion problem, we modified our shock tube to allow injection of gases into the supersonic flow behind an incident shock wave. We employ a pulsed valve, with a 2 mm round orifice, which was custom-built to allow rapid opening. Tests have been conducted with nonreacting and reacting jets. In the nonreacting case, a jet of 5% NO in $N_2$ was injected into a freestream of 21% $N_2$ in argon, while in the reacting flow study the jet was pure $H_2$ and the freestream was 21% $O_2$ in argon. In both cases, the jet stagnation conditions were nominally 300K and 3.4 atm, the freestream Mach number was 1.4 and the freestream static temperature and pressure were 2100K and 0.39 atm, respectively. Imaging measurements of NO, in the nonreacting case, essentially represent the jet mixture mole fraction, the quantity of primary interest in characterizing the mixing of the jet fluid. In the case of the reacting jet, we imaged OH, which essentially is an indicator of the flame front. In our most recent work, we utilized two laser sources and two CCD cameras, thereby obtaining two nearly simultaneous images useful either for single-shot imaging of two species on temperature.

A sketch of the generic flowfield is provided in Fig. 12. Sample results (centerline images along the shock tube axis) for the nonreacting case (both single-shot and time-averaged) are shown in Fig. 13. Note particularly the presence of large-scale structures in the instantaneous image; these features of course disappear in the time-averaged data. We believe that these structures are likely to play a key role in the mixing of high-speed jets, and yet their presence is not accounted for in current models (usually time-averaged) of jet mixing. Finally, a comparison of end-view images of the nonreacting and reacting cases is shown in Fig. 14. The OH image shows that the flame front is nearly round in this view, surrounding the unburned fuel jet. The nonreacting case, by contract, has no hollow core since the quantity being monitored is representative of the jet fluid. Also, note the evidence at this axial location of interaction between the jet fluid and the wall boundary layer.

These images, which represent the first single-shot PLIF data for this important flow, validate our strategy of utilizing a shock tube as a convenient, economical vehicle for generating scramjet flows. More recently we have published the first two-laser, two-camera PLIF data for these flows. These images can be deployed to give either instantaneous temperature fields or simultaneous measurements of two species, typically OH and NO.

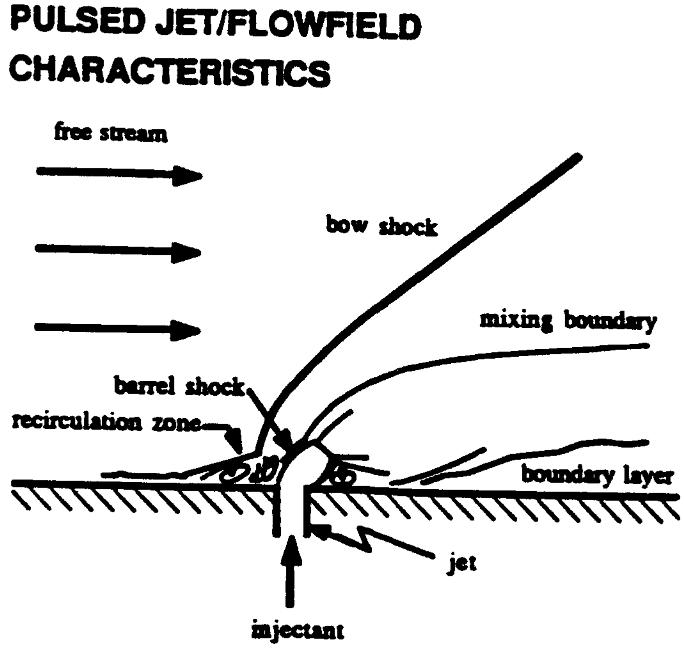


**Fig. 12. Schematic of the flowfield, illustrating the characteristic flow features.**

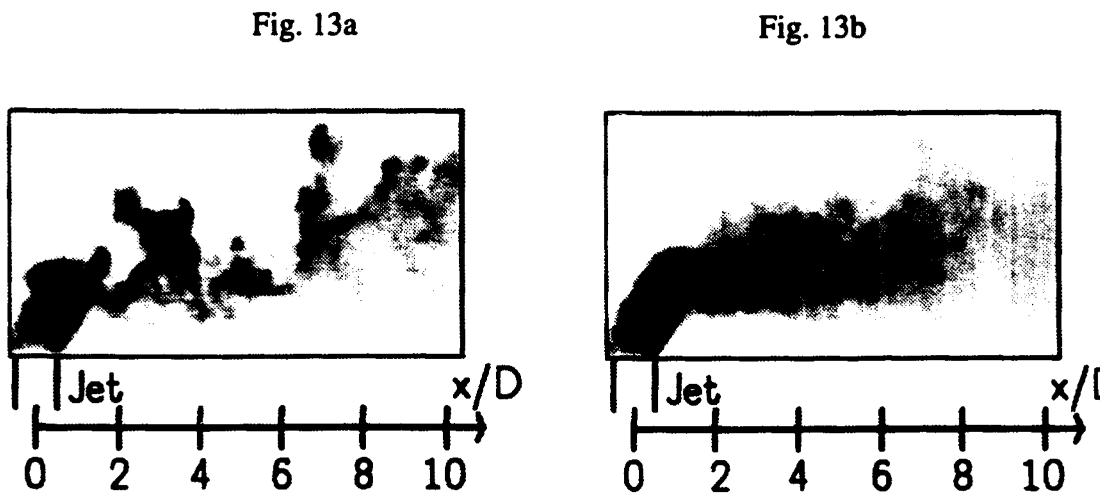


**Fig. 13. PLIF images of NO acquired in the side-view geometry displayed in Fig. 9. (a) Single-shot PLIF of NO. (b) 12-frame average PLIF image of NO. Signal is presented in a continuous gray scale, where white indicates low signal and black indicates high signal. The imaged area is 22 × 22 mm trimmed down to 11 × 22 mm, and extends from x/D = -1 to x/D = 10 in the axial direction.**

Fig. 14a

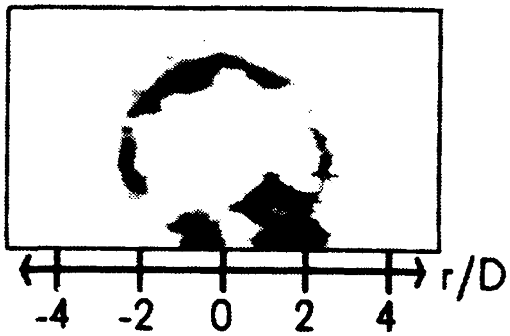


Fig. 14b

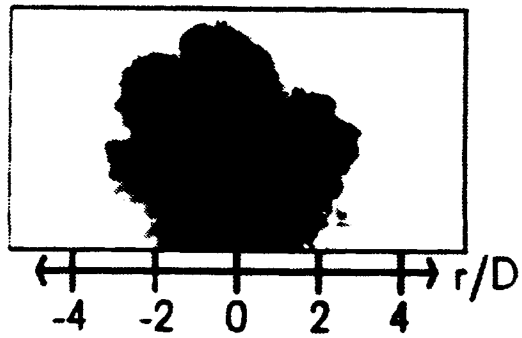


**Fig. 14. End-view PLIF images of NO and OH at an axial location x/D = 15. (a) Single-shot PLIF image of OH. (b) Single-shot image of NO. The imaged region shown is 11 × 22 mm.**

## 5.0 STABILITY ANALYSIS AND NUMERICAL SIMULATIONS

### 5.1 Objective

The objective of this phase of the program is to use stability analysis and numerical simulations to gain insight into the physical structure and mixing physics in a supersonic mixing layer between chemically reactive streams.

### 5.2 Research Results

A summary of the significant results of the stability analyses and numerical simulations is given below:

The dominance of three-dimensional modes in high-speed non-reacting mixing layers was demonstrated (Sandham and Reynolds 1989). This led to early modifications of the experimental apparatus to enable three-dimensional viewing. In addition, a simple formula for the dominant instability mode angle for non-reacting mixing layers was developed (Sandham and Reynolds 1990), in terms of the convective Mach number $M_c$:

$$M_c \cos(\theta) = 0.6$$

The concept of the *flame convective Mach number*, as the important parameter controlling instability in reacting mixing layers, was introduced (Planche and Reynolds 1991a, 1991b, 1992a).

We demonstrated that the obliquity angle formula of Sandam and Reynolds, developed for non-reacting mixing layers, holds very well for reacting flows if $M_c$ is replaced by the flame convective Mach number $M_f$ (Planche and Reynolds 1992b).

The appearance of a colayer structure in high-speed reacting mixing layers was forecast (Planche and Reynolds 1992a, 1992b); see Fig. 15. This led to proposals for new experimental research.

The mechanism of transition to small-scale turbulence in high-speed reacting mixing layers was identified (Planche and Reynolds 1992b).

Results from initial direct numerical simulations suggest that streamwise vortices may enhance the mixing and combustion in supersonic mixing layers (Planche and Reynolds 1991b, 1992a, 1992b).

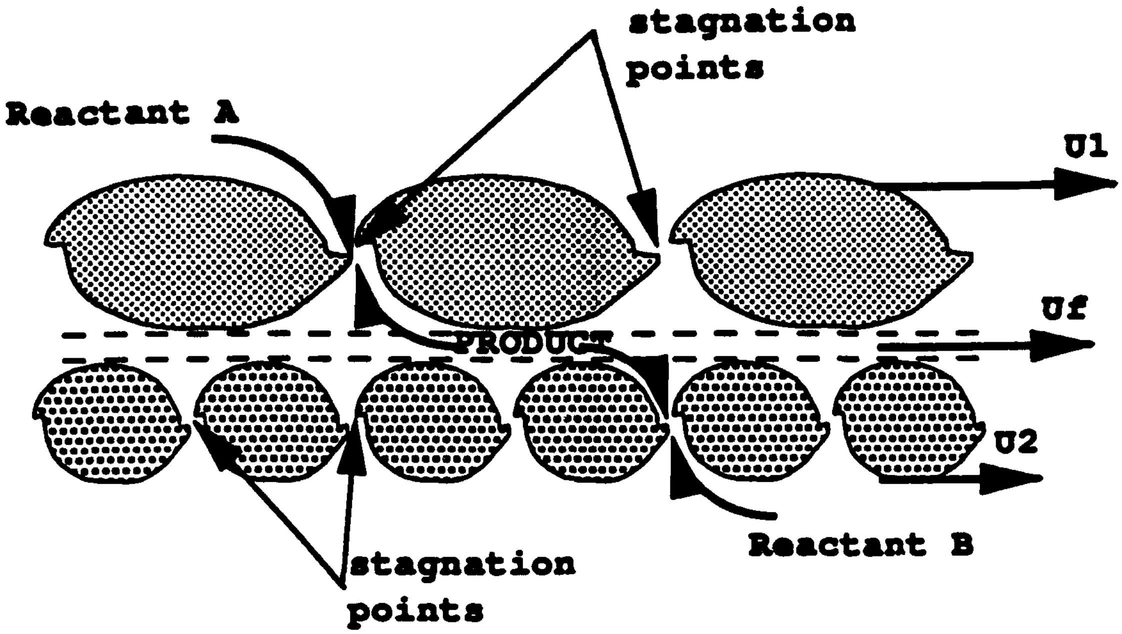


**Fig. 15. Schematic of the compressible reacting mixing layer.**

### 5.3 Colayer Structure

Figure 15 shows what is probably the most surprising and new result from this phase of the program: the forecast of the appearance of *colayers* in a high-speed reacting mixing layer. The stability analysis showed that the dominant instability modes are determined by the peaks in the profile of the product of the mean density (ρ) and mean vorticity (dU/dy). In an incompressible mixing layer, this profile has a single peak near the center of the mixing layer, and gives rise to a single train of two-dimensional vortices that move at a phase speed of approximately the mean velocity in the center of the layer (the familiar Brown/Roshko vortices). In a reacting mixing layer, the region of low density at the flame sheet produces a dip in the ρdU/dy profile, with a strong peak on either side of the flame. Spanwise vortices are formed near the peaks on both sides of the flame.

These two rows of vortices form two parallel mixing layers (the *colayers*). The vortices in each layer move at a phase speed that is approximately the mean velocity at the peak on its side of the flame sheet, so that the high-speed vortices slip past those on the low-speed side with little interaction. The two layers behave very independently, and pairing events are very rare on either side. One of the colayers mixes the fuel stream with product from the combustion, and the other mixes the oxidizer stream with product, but there is no direct mixing of fuel and oxidizer.

This prediction from our stability analysis was confirmed by our full non-linear direct numerical simulation for temporally developing reacting mixing layers. In a planned future program at Stanford, experiments will be conducted to determine if this very unusual structure occurs in actual spatially-developing mixing.

Our numerical simulations showed that small-scale transition occurs independently in each of the colayers, and results in intense streamwise vortices in the braid regions of each layer. These enhance the reaction rate. This suggests that the rate of combustion in a supersonic mixing layer can be increased significantly by increasing the streamwise vorticity in the flow. Future experiments and simulations will explore this further.

## 6.0 PRESENTATIONS AND PUBLICATIONS

### 6.1 Presentations

P. H. Paul, M. P. Lee, B. K. McMillin, J. M. Seitzman and R. K. Hanson (1990), "Application of Planar Laser-Induced Fluorescence Imaging Diagnostics to Supersonic Reacting Flow," paper 90-1844 at 28th AIAA/SAE/ASME/ASEE Joint Propulsion Conf., Orlando, FL.

R. K. Hanson, A. Y. Chang, M. D. DiRosa, L. C. Philippe, B. K. McMillin and M. P. Lee (1990), "Laser-Based Diagnostics for Propulsion and Hypersonics Testing," paper AIAA-90-1383 presented at AIAA 16th Aerodynamic Ground Testing Conf., Seattle WA.

B. K. McMillin, P. H. Paul and R. K. Hanson (1990), "Planar Laser-Induced Fluorescence Imaging of Nitric Oxide in Shock Tube Flows with Vibrational Nonequilibrium," paper AIAA-90-1519 at AIAA 21st Fluid Dynamics, Plasmadynamics and Lasers Conf., Seattle WA.

J. L. Palmer, B. K. McMillin and R. K. Hanson (1991a), "Planar Laser-Induced Fluorescence Imaging of Underexpanded Free Jet Flow in a Shock Tunnel Facility," AIAA 22nd Fluid Dynamics, Plasma Dynamics and Lasers Conference, Honolulu, HI.

B. K. McMillin, M. P. Lee, J. L. Palmer and R. K. Hanson (1991a), "Two-Dimensional Temperature Measurements of Nonequilibrium Supersonic Flows Using Planar Laser-Induced Fluorescence of Nitric Oxide," paper AIAA-91-1670 at AIAA 22nd Fluid Dynamics, Plasma Dynamics and Lasers Conference, Honolulu, HI.

J. L. Palmer, B. K. McMillin and R. K. Hanson (1991b), "Planar Laser-Induced Fluorescence Imaging of Underexpanded Free Jet Flow in a Shock Tunnel Facility," paper AIAA-91-1687 at AIAA 22nd Fluid Dynamics, Plasma Dynamics and Lasers Conference, Honolulu, HI.

B. K. McMillin, M. P. Lee, J. L. Palmer and R. K. Hanson (1991b), "Two-Dimensional Imaging of Shock Tube Flows Using Planar Laser-Induced Fluorescence," presented at 18th International Symposium on Shock Waves, Sendai, Japan.

O. H. Planche and W. C. Reynolds (1991a), "Compressibility effects on the supersonic reacting mixing layer", AIAA 91-0739.

J. L. Palmer, B. K. McMillin and R. K. Hanson (1992), "Planar Laser-Induced Fluorescence Imaging of Velocity and Temperature in Shock Tunnel Flows," paper AIAA 92-0762, AIAA 30th Aerospace Sciences Meeting, Reno.

O. H. Planche and W. C. Reynolds (1992a), "Heat Release Effects on Mixing in Supersonic Mixing Layers," AIAA-92-0092.

B. K. McMillin, J. L. Palmer and R. K. Hanson (1992a), "Instantaneous 2-D Temperature Measurements of Shock Tube Flows using Laser-Induced Fluorescence of Nitric Oxide," presented at Measurement Technology Conf., NASA Langley Res. Ctr.

B. K. McMillin, J. L. Palmer and R. K. Hanson (1992b), "Instantaneous 2-D Temperature Measurements of a Transverse Jet in a Shock-Heated Supersonic Crossflow," paper AIAA-92-3347 at $20^{th}$ AIAA/SAE/ASME/ASAE Joint Propulsion Conference, Nashville, July 6-8, 1992.

M. F. Miller, T. C. Island, B. Yip, C. T. Bowman, M. G. Mungal and R.K. Hanson (1993a), "An Experimental Study of the Structure of a Compressible, Reacting Mixing Layer," AIAA-93-0354, presented at 31st AIAA Aerospace Sciences Meeting, Reno, NV.

Miller, M.F., Island, T.C., Seitzman, J.M., Mungal, M.G., Bowman, C.T. and R.K. Hanson (1993b), "Compressibility Effects in a Reacting Mixing Layer," AIAA-93-1771, presented at 29th AIAA/SAE/ASME/ASEE Joint Propulsion Conference, Monterey, CA.

### 6.2 Publications

B. K. McMillin, M. P. Lee, P. H. Paul and R. K. Hanson (1990), "Planar Laser-Induced Fluorescence Imaging of Shock-Induced Ignition," *Twenty-Third Symposium (International) on Combustion*, The Combustion Institute, 1909-1914.

N. D. Sandham and W. C. Reynolds (1990), "The Compressible Mixing Layer: Linear Theory and Direct Simulation". AIAA J., **28**, 618-624.

N. T. Clemens and M. G. Mungal (1991), "A Planar Laser Mie Scattering Technique for Visualizing Supersonic Mixing Flows," Expts. in Fluids **11**, 175-185.

N. D. Sandham and W. C. Reynolds (1991a), "Three-Dimensional Simulations of Large Eddies in the Compressible Mixing Layer," J. Fluid Mech. **224**, 133-158.

O. H. Planche and W. C. Reynolds (1991b), "Direct Simulation of a Supersonic Reacting Mixing Layer". *8th Symposium on Turbulent Shear Flows*, 21-1, Munich, Germany.

N. T. Clemens and M. G. Mungal (1992a), "Two- and Three-Dimensional Effects in the Supersonic Mixing Layer," AIAA J. **30**, 973-981.

N. T. Clemens and M. G. Mungal (1992b), "Effects of Sidewall Disturbances on the Supersonic Mixing Layer," J. Prop. Power **8**, 249-251.

L. C. Cohen and R. K. Hanson (1992), "Emission and Laser-Induced Fluorescence Measurements in a Supersonic Jet of Plasma-Heated Nitrogen," J. Phys. D: Applied Phys. **25**, 339-351.

M. P. Lee, B. K. McMillin, J. L. Palmer and R. K. Hanson (1992), "Two-Dimensional Imaging of a Transverse Jet in Supersonic Crossflow," J. Prop. and Power **8**, 729-735.

B. K. McMillin, M. P. Lee, J. L. Palmer and R. K. Hanson (1992), "Two-Dimensional Imaging of Shock Tube flows Using Planar Laser-Induced Fluorescence," *Shock Waves*, Proceedings of 18th Shock Tube Symposium, T. Takayama (ed.), Springer-Verlag, pp. 819-824.

O. H. Planche and W. C. Reynolds (1992b), "A Direct Numerical Simulation of the Compressible Reacting Mixing Layer". *Parallel CFD 92*, New Brunswick, NJ.

R. K. Hanson (1992), "Laser-Based Diagnostics for Hypersonic Flows," in *New Trends in Instrumentation for Hypersonic Research*, A. Boutier (ed.), NATO ASI, Series E-Vol. 224, Kluwer Academic Publishers, The Netherlands, pp. 185-194.

B. K. McMillin, J. L. Palmer and R. K. Hanson (1992), "Instantaneous Temperature Imaging of a $H_2$/NO Jet in Supersonic Crossflow Using Two-Line PLIF," Applied Optics, submitted.

B. Yip, M. F. Miller, A. Lozano and R.K. Hanson (1993), "A Combined OH/Acetone Planar Laser-Induced Fluorescence Imaging Technique for Visualizing Combusting Flows," submitted for publication to Experiments in Fluids.

B. K. McMillin, J. M. Seitzman, J. L. Palmer and R. K. Hanson (1993), "Dual-Laser PLIF Imaging Techniques for Shock Tube Studies of Mixing and Combustion," 19th Int. Symp. on Shock Waves (ISSW 19), Marseille.

J. M. Seitzman, M. F. Miller, T. C. Island and R. K. Hanson (1994), "Double-Pulsed Imaging Using Simultaneous Acetone/OH PLIF for Studying the Evolution of High-Speed, Reacting Mixing Layers," submitted for publication to The Combustion Institute for the 25th Symposium (International) on Combustion, Irvine, CA.

## 7.0 PERSONNEL

| | |
|---|---|
| Craig T. Bowman | Professor, Mechanical Engineering |
| Ronald K. Hanson | Professor, Mechanical Engineering |
| Mark Godfrey Mungal | Associate Professor, Mechanical Engineering |
| William C. Reynolds | Professor, Mechanical Engineering |
| Gregory A. Blaisdell | Graduate Research Assistant, Mechanical Engineering |
| Noel T. Clemens | Graduate Research Assistant, Mechanical Engineering |
| Tobin Island | Graduate Research Assistant, Mechanical Engineering |
| Michael P. Lee | Graduate Research Assistant, Mechanical Engineering |
| Brian McMillin | Graduate Research Assistant, Mechanical Engineering |
| Michael F. Miller | Graduate Research Assistant, Mechanical Engineering |
| Olivier Planche | Graduate Research Assistant, Mechanical Engineering |
| Jennifer Palmer | Graduate Research Assistant, Mechanical Engineering |
| William D. Urban | Graduate Research Assistant, Mechanical Engineering |

## 8.0 Ph.D. DEGREES AWARDED

N. D. Sandham, 1989, "A Numerical Investigation of the Compressible Mixing Layer."

Lawrence Cohen, 1990, "Emission and Laser-Induced Fluorescence Diagnostics of a Supersonic Jet of Plasma-Heated Nitrogen."

Noel Clemens, 1991, "An Experimental Investigation of Scalar Mixing in Supersonic Turbulent Shear Layers."

Michael Lee, 1991, "Temperature Measurements in Gases Using Planar Laser-Induced Fluorescence Imaging of NO and $O_2$."

O. H. Planche, 1992, "A Numerical Investigation of the Compressible Reacting Mixing Layer."

Brian McMillin, 1993, "Instantaneous Two-Line PLIF Temperature Imaging of Nitric Oxide in Supersonic Mixing and Combustion Flowfields."